# $N^G$-Aminoguanidines from Primary Amines and the Preparation of Nitric Oxide Synthase Inhibitors

Nathaniel I. Martin,† William T. Beeson, Joshua J. Woodward, and Michael A. Marletta*

*Departments of Chemistry, Molecular and Cellular Biology, and Division of Physical Sciences, Lawrence Berkeley National Laboratory, University of California, Berkeley, Berkeley, California 94720-3220*

*Received September 9, 2007*

A concise, general, and high-yielding method for the preparation of $N^G$-aminoguanidines from primary amines is reported. Using available and readily prepared materials, primary amines are converted to protected $N^G$-aminoguanidines in a one-pot procedure. The method has been successfully applied to a number of examples including the syntheses of four nitric oxide synthase (NOS) inhibitors. The inhibitors prepared were investigated as competitive inhibitors and as mechanistic inactivators of the inducible isoform of NOS (iNOS). In addition, one of the four inhibitors prepared, $N^G$-amino-$N^G$-2,2,2-trifluoroethyl-L-arginine **19**, displays the unique ability to both inhibit NO formation and prevent NADPH consumption by iNOS without irreversible inactivation of the enzyme.

## Introduction

$N^G$-Aminoguanidines have been of medicinal interest for some time and have been previously described as anticancer, antibacterial, and antiviral agents.[1,2] This class of compounds also display dopamine $\beta$-oxidase inhibition and antihypertensive properties.[3] Substituted aminoguanidines have been shown to inhibit the advanced nonenzymatic glycosylation of proteins[4,5] and arylaminoguanidines have been described as a novel class of 5-HT2aA receptor antagonists.[6] Recent work has also suggested that $N^G$-aminoguanidine functionalities can be utilized in the design of potent inhibitors for trypsin-like serine proteases.[7,8] Our interest in these compounds stems from our continuing work with the nitric oxide synthases (NOSs[a], EC 1.14.13.39) and previous reports that certain $N^G$-aminoguanidines inhibit NOS activity.[9,10] The NOSs are a family of enzymes that catalyze the conversion of L-arginine to L-citrulline and nitric oxide (NO) via the intermediate $N^G$-hydroxy-L-arginine (NHA; Scheme 1).[11,12] NOSs are active as homodimers, with each subunit containing a C-terminal reductase domain (with binding sites for NADPH, FAD, and FMN) and an N-terminal oxygenase domain containing the heme prosthetic group. The substrate, L-arginine, and a redox cofactor, (6*R*)-5,6,7,8 tetrahydro-L-biopterin ($H_4B$), both bind near the heme center in the oxygenase domain.[13]

NO regulates numerous physiological processes, including neurotransmission, smooth muscle relaxation, platelet reactivity, and the cytotoxic activity of immune cells.[14] Overproduction of NO has been linked to the pathogenesis of a number of disease states, including septic shock, neurodegenerative disorders, and inflammation.[15] For this reason, compounds capable of inhibiting the NOSs, including $N^G$-aminoguanidines, remain of interest.

**Scheme 1.** Reaction Catalyzed by NOS

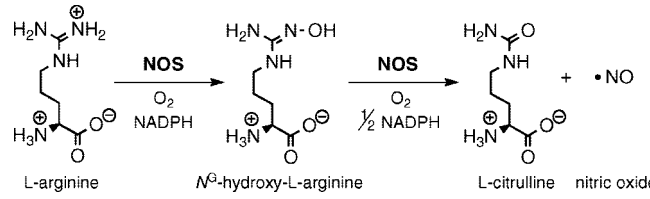


Despite the widespread interest in $N^G$-aminoguanidines, few general methods have been developed by which these functionalities can be conveniently and safely constructed under mild conditions. Traditional approaches involve the use of toxic reagents and harsh reaction conditions and have generally relied upon the addition of hydrazines to cyanimides (prepared by CNBr treatment of the starting amine)[16,17] or to thioureas requiring preactivation with $HgCl_2$, PbO, or alkyl iodides.[18,19] Recently, Katritzky and co-workers described an alternate route to $N^G$-aminoguanidines via treatment of di(benzotriazol-1-yl)methanimine with the appropriate amines and hydrazines in refluxing toluene.[20]

As mentioned above, $N^G$-aminoguanidine containing compounds have also been described as inhibitors of NOS.[9] $N^G$-Amino-L-arginine is a well-known irreversible inhibitor of NOS and exhibits mechanism-based, time-dependent inactivation of the enzyme.[21] The nature of this inactivation has been previously investigated and has been shown to be the result of a covalent modification of the enzyme. Based on mass spectrometric evidence, Osawa and co-workers have proposed a modification pathway whereby the inhibitor is converted to a reactive intermediate by the action of NOS itself.[22] This reactive species then covalently cross-links with the heme prosthetic group, resulting in a catalytically inactive form of the enzyme (Scheme 2). Whether this heme-modification pathway is a general mechanism by which $N^G$-aminoguanidines inhibit NOS is

* To whom correspondence should be addressed. Departments of Chemistry and Molecular and Cellular Biology, and Division of Physical Sciences, Lawrence Berkeley National Laboratory, University of California, Berkeley, 570 Stanley Hall, Berkeley, CA 94720-3220. Tel.: (510) 666-2763. Fax: (510) 666-2765. E-mail: marletta@berkeley.edu.

† Current address: Department of Medicinal Chemistry and Chemical Biology, Utrecht University, F.A.F.C. Wentgebouw, Room Z615, Sorbonnelaan 16, 3584 CA Utrecht, The Netherlands.

[a] Abbreviations: NOS, nitric oxide synthase; iNOS, inducible NOS; $iNOS_{heme}$, heme domain of inducible NOS; $H_4B$, (6*R*)-5,6,7,8-tetrahydro-L-biopterin; NADPH, nicotinamide adenine dinucleotide phosphate; FAD, flavin adenine dinucleotide; FMN, flavin monomucleotide; CbZNCS, *N*-benzyloxycarbonyl isothiocyanate; OxyMb, oxymyoglobin; DTT, dithiothreitol; HEPES, 4-(2-hydroxyethyl)-1-piperazineethane sulfonic acid.

10.1021/jm701119v CCC: $40.75 
Published on Web 01/26/2008

**Scheme 2.** Proposed Inactivation of NOS by $N^G$-Amino-L-arginine[22]

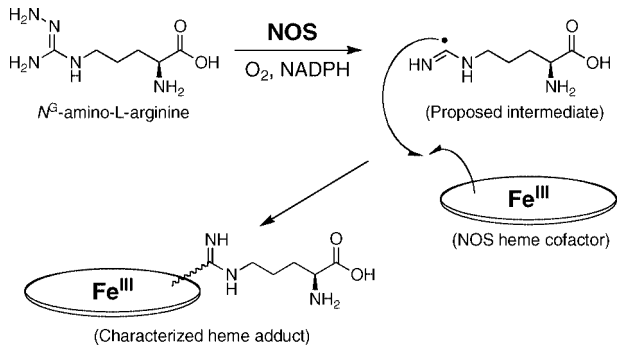


unknown and presented an additional motivation for our investigation.

## Results and Discussion

An initial objective in our investigation was the development of a convenient and general approach for the synthesis of $N^G$-aminoguanidines. While the addition of nucleophiles to thioureas has been previously described in this regard,[18,19] the lack of suitable protecting groups along with the use of toxic reagents and harsh coupling conditions has somewhat limited the generality of these approaches. We recently described the preparation and use of *N*-benzyloxycarbonyl isothiocyanate (CbzNCS) in the conversion of amines to protected $N^G$-hydroxyguanidines via thiourea intermediates. The thiourea intermediates need not be isolated and are readily converted to protected $N^G$-hydroxyguanidines in a high-yielding, one-pot procedure.[23] We have found that a similar approach, whereby Cbz-protected thioureas are activated with *N*-(3-dimethylaminopropyl)-*N*-ethylcarbodiimide hydrochloride (EDCI) and treated with benzyl carbazate, is of equal generality in the synthesis of $N^G$-aminoguanidines (Scheme 3).

**Scheme 3.** One-Pot Preparation of $N^G$-Aminoguanidines

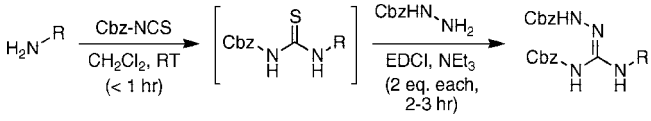


The strategy illustrated in Scheme 3 was successfully applied to a variety of amines. The expected Cbz-protected $N^G$-aminoguanidine products were all rapidly formed at room temperature and in good yields (Table 1). A practical advantage of this approach is that the $N^G$-hydroxyguanidine moiety is installed in a fully Cbz-protected form, allowing for purification by standard chromatographic techniques prior to deprotection. While previously reported syntheses of $N^G$-aminoguanidines have provided the target molecules directly, the lack of protecting groups can complicate purification owing to the high polarity of such compounds. In addition, $N^G$-aminoguanidines are stable to reductive conditions, allowing for global removal of the Cbz groups by standard hydrogenation to directly yield the fully deprotected products (see below for further examples and description of deprotection conditions). It should be noted, however, that it is not possible to convert secondary amines to the corresponding $N^G$-aminoguanidines using this procedure. The EDCI-mediated coupling likely occurs via the formation of a transient carbodiimide[24] not attainable with secondary amines. In cases where $N^G$-aminoguanidines derived from secondary amines are required, the approach of Katritzy and co-workers presents a viable alternative.[20]

**Table 1.** Cbz-Protected $N^G$-Aminoguanidines Prepared

| Entry | amine | product | yield (%)[a] |
|---|---|---|---|
| 1 | 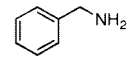 | 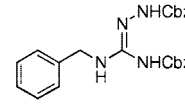 | 97 |
| 2 | 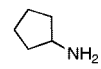 | 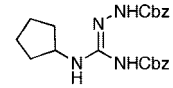 | 95 |
| 3 |  | 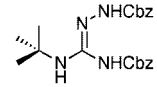 | 94 |
| 4 | 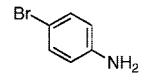 | 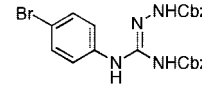 | 91 |
| 5 | 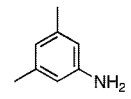 | 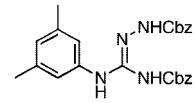 | 96 |
| 6[b] | 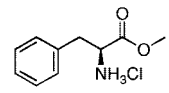 | 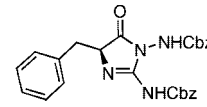 | 89 |

[a] Isolated yield. [b] An equivalent of $NEt_3$ added to the amine hydrochloride prior to treatment with CbzNCS.

After establishing the validity of this approach for the preparation of the $N^G$-aminoguanidine core, the methodology was further applied to the preparation of four L-arginine analogues to be investigated as inhibitors of iNOS. The four L-arginine analogues were designed to probe the role of both electron-rich and electron-poor substituents located at either of the two amino positions originally deriving from the hydrazine used in constructing the $N^G$-aminoguanidine center. Benzyl carbazate as well as the commercially available 2,2,2-trifluoroethyl- and monomethyl-substituted hydrazines were used as starting materials to yield the four analogues each deriving from the same thiourea precursor **8**. The orthogonally protected L-ornithine species **7** was first prepared by standard means and converted to **8** by TFA deprotection, followed by treatment with CbzNCS (Scheme 4).

**Scheme 4.** Preparation of Thiourea **8**

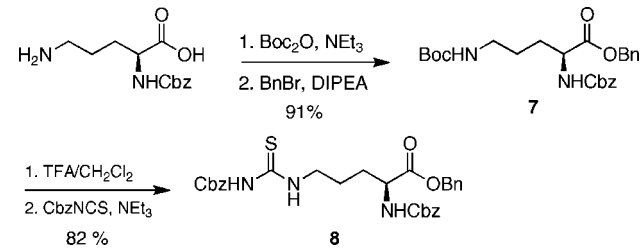


The required hydrazines were then Cbz-protected using standard carbamate chemistry (Scheme 5). In choosing the position for the Cbz protecting group on the hydrazine, it is possible to dictate the substitution pattern in the final $N^G$-aminoguanidine product. Compound **9** was prepared by direct treatment of methylhydrazine with CbzCl leading to carbamate

**Scheme 5.** Preparation of Cbz-Protected Methyl and 2,2,2-Trifluoroethylhydrazines

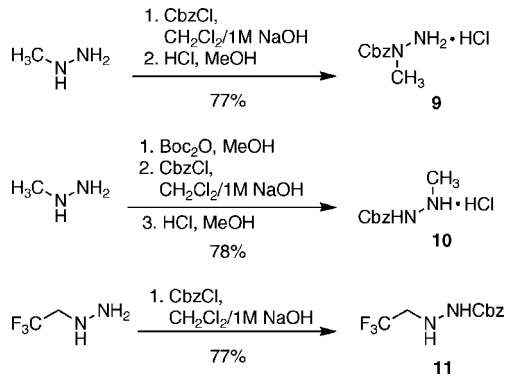


protection at the more nucleophilic (methylated) nitrogen. When methylhydrazine was first treated with $Boc_2O$ followed by CbzCl, the Cbz group was installed at the less nucleophilic nitrogen. Acid treatment to remove the Boc carbamate then yielded compound **10**. Compound **11** was obtained by treating 2,2,2-trifluoroethylhydrazine with CbzCl. In this case, the electron withdrawing effect of the trifluoromethyl group led to preferential protection of the less-substituted nitrogen.

The four Cbz-protected $N^G$-amino-L-arginine analogues **12**−**15** were then prepared by treatment of thiourea **8** with EDCI, $NEt_3$, and the appropriate Cbz-protected hydrazine (Scheme 6). Deprotection of **12**−**15** was accomplished by hydrogenation over Pd/C to provide the amino acid products **16**−**19** as the acetate salts after lyophilization (with the exception of compound **18**, which was isolated as the free base after lyophilization. as evidenced by NMR; Scheme 6).

**Scheme 6.** Preparation of Amino Acid Products **16–19**

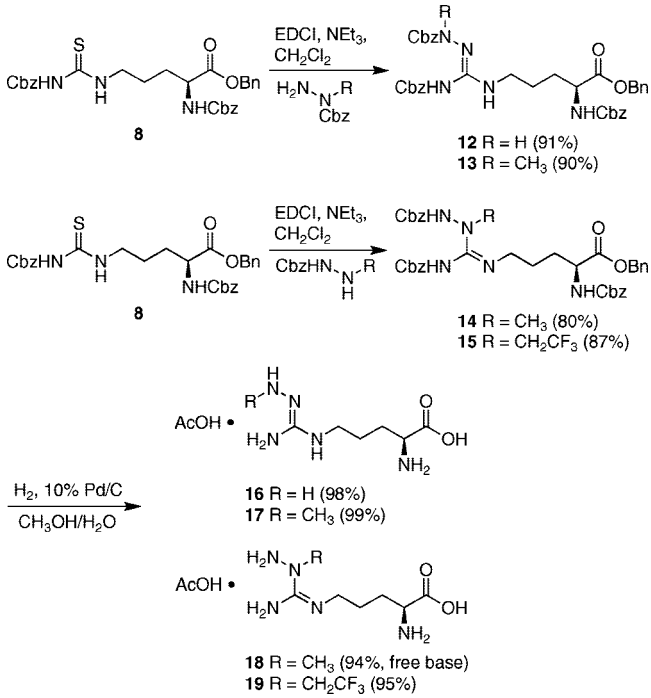


NOS binding affinities for the four $N^G$-amino-L-arginine analogues were determined using a previously described spectral binding assay.[25] For this analysis, a truncated construct of iNOS ($iNOS_{heme}$, comprised of amino acids 1–490) was used. This construct has been previously shown to bind heme, $H_4B$, and substrate(s) in identical fashion to the full-length enzyme and is catalytically competent when provided with an exogenous source of electrons such as sodium dithionite.[25] Addition of **16**−**19** to $H_4B$-bound $iNOS_{heme}$ induced a low- to high-spin state conversion at the heme center resulting from loss of water ($Fe^{III}$-aqua → $Fe^{III}$-unligated) upon binding. This transition leads to a decrease in absorbance at ∼418 nm and an increase in absorbance at ∼394 nm in the UV–visible spectrum. The magnitude of spectral change, ΔΔAbs (where $\Delta\Delta Abs = \Delta Abs_{394} - \Delta Abs_{418}$), is dependent on the concentration of the added analogue. Spectral $K_d$ values for each compound are then determined by fitting the titration data to the saturation binding equation: $\Delta\Delta Abs = (\Delta\Delta Abs_{max} \times [compound])/(K_d + [compound])$. Table 2 summarizes the spectral binding assay results for compounds **16**−**19** (graphic depictions of the titration experiments for all four analogs provided in Supporting Information).

**Table 2.** Spectral $K_d$ Values for **16–19**

| compound | spectral $K_d$[a] ($\mu$M) |
|---|---|
| L-arginine[b] | 7.0 ± 0.7 (5.8 ± 1.6) |
| $N^G$-amino-L-arginine (**16**) | 1.3 ± 0.2 |
| $N^G$-methylamino-L-arginine (**17**) | 29.0 ± 2.5 |
| $N^G$-amino-$N^G$-methyl-L-arginine (**18**) | 10.0 ± 0.5 |
| $N^G$-amino-$N^G$-2,2,2-trifluoroethyl-L-arginine (**19**) | 40.4 ± 3.8 |

[a] Spectral $K_d$ values reported for **16–19** are averages obtained from triplicate analysis. [b] Previously reported value given in parentheses.[25]

Next, compounds **16–19** were examined as inhibitors for full-length iNOS. NOS activity was measured using a spectral assay making use of the NO-induced oxidation of oxymyoglobin to metmyoglobin observable at 405 nm. Table 3 lists the $K_i$ values determined for compounds **16–19** (with graphic depictions of the iNOS inhibition assays for all four analogs provided in Supporting Information).

**Table 3.** $K_i$ Values Determined for **16–19**

| compound | $K_i$[a] ($\mu$M) |
|---|---|
| $N^G$-amino-L-arginine (**16**)[b] | 2.2 ± 0.5 (1.7 ± 0.6) |
| $N^G$-methylamino-L-arginine (**17**) | 16.4 ± 5.0 |
| $N^G$-amino-$N^G$-methyl-L-arginine (**18**) | 34.1 ± 7.2 |
| $N^G$-amino-$N^G$-2,2,2-trifluoroethyl-L-arginine (**19**) | 10.5 ± 5.7 |

[a] Values reported are averages obtained from triplicate analysis. [b] Previously reported value given in parentheses.[26]

Compounds **16–19** were next investigated as time-dependent inactivators of iNOS. Each compound was used at a concentration 10-fold higher than the measured $K_i$ and allowed to react with iNOS under turnover conditions (NADPH, $H_4B$, $O_2$). Time points were obtained by quenching aliquots from each reaction mixture into a concentrated L-arginine solution (final concentration of L-arginine 100-fold higher than compound tested). The oxymyoglobin assay was then used to measure residual iNOS activity as a function of preincubation time with **16–19**. Of the four compounds tested, only $N^G$-amino-L-arginine **16** (as expected[21]) and $N^G$-amino-$N^G$-methyl-L-arginine **18** displayed an ability to irreversibly inactivate iNOS in a time-dependent manner. $K_{inactivation}$ values were determined by plotting residual iNOS activity as a function of preincubation time (Figure 1). The $K_{inactivation}$ value measured for $N^G$-amino-L-arginine **16** was $0.18 \pm 0.01$ min$^{-1}$ (compared to a previously reported value[21] of 0.26 min$^{-1}$). Compound **18** inactivates iNOS at a higher rate with a measured $K_{inactivation}$ value of $0.39 \pm 0.02$ min$^{-1}$.

As mentioned above, Osawa and co-workers have shown that $N^G$-amino-L-arginine inactivates NOS by covalent modification of the heme cofactor.[22] To investigate whether or not a heme

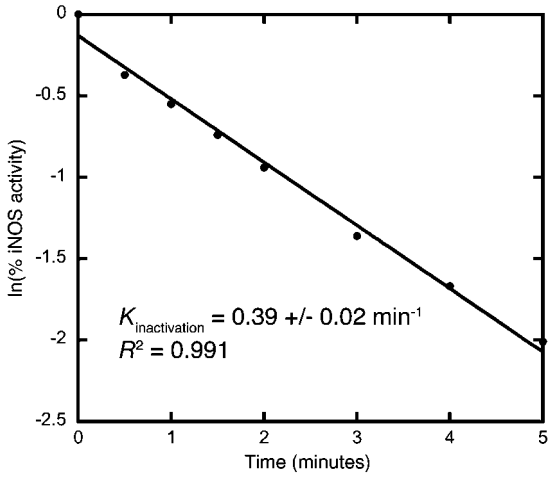


**Figure 1.** Time-dependent inactivation of iNOS by **18**.

modification mechanism was responsible for the iNOS inactivation observed with **18**, a mass spectral analysis was used. iNOS was reacted with either $N^G$-amino-L-arginine or compound **18** in the presence of NADPH for 30 min after which the heme content of the samples was assessed by LC-MS. While treatment of iNOS with $N^G$-amino-L-arginine led to formation of the expected adduct[22] (MW = 775.3), no modified heme species were detected in iNOS samples treated with **18**. This suggests that heme modification is not an inactivation pathway common to all $N^G$-aminoguanidine-based inhibitors of NOS. The irreversible iNOS inactivation caused by compound **18** is possibly due to modification of an amino acid(s) in the enzyme active site.

Compounds **17** and **19** were shown not to be time-dependent inactivators of iNOS and were further examined for an ability to inhibit iNOS-mediated NADPH oxidation (Figure 2). The rate at which NADPH is oxidized by NOS is regulated by a number of factors[27] and in the absence of L-arginine the enzyme consumes NADPH (Figure 2, basal activity) to generate reactive oxygen species like superoxide and peroxide.[27,28] While incubation with compound **17** led to no significant difference versus the basal rate (no L-arginine present) of iNOS-mediated NADPH consumption, compound **19** severely inhibited NADPH oxidase activity.

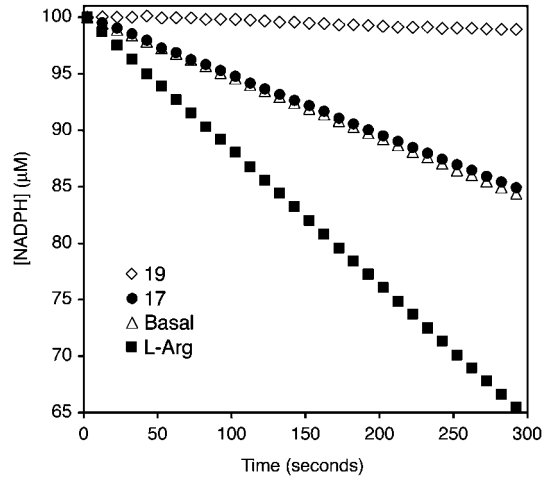


**Figure 2.** Effect of **17** and **19** on iNOS-mediated NADPH consumption. Compound **17** has little impact on the rate of NADPH consumption by iNOS (similar to basal oxidation rate). Compound **19** causes a significant decrease in the observed rate of NADPH oxidation (<5% of the rate observed with L-arginine).

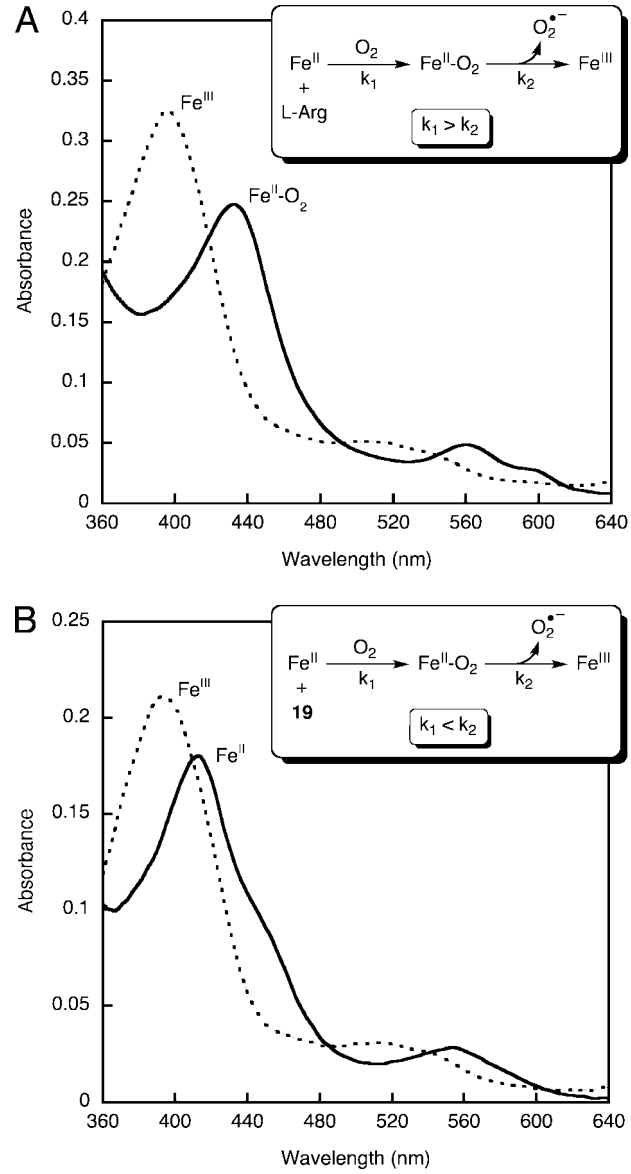


**Figure 3.** Extracted spectral intermediates observed for heme transitions from stopped-flow UV–visible spectroscopic analysis. Oxidation of $iNOS_{heme}$ containing $H_2B$ in the presence of (A) L-arginine or (B) compound **19**.

To further elucidate the nature of the inhibition of iNOS-mediated NADPH consumption by compound **19**, stopped-flow rapid-scanning UV/visible spectroscopic analyses were performed. As previously described,[29,30] the introduction of oxygen to $Fe^{II}$-$iNOS_{heme}$ (reconstituted with redox-inactive (6*R*)-7,8-dihydro-L-biopterin ($H_2B$) and premixed with L-arginine) results in a rapid conversion of the ferrous protein to the ferrous-oxy complex, followed by the appearance of high-spin ferric protein due to the dissociation of superoxide from the heme. Under our experimental conditions, oxygen binding occurs at a rate that was not resolvable, resulting in no observable ferrous starting protein (Figure 3A). The data fit well to an A → B kinetic model in which dissociation of superoxide is clearly observed as a transition of an intermediate with a Soret absorbance at 428 nm ($Fe^{II}$-$O_2$) to a species at 396 nm ($Fe^{III}$) with a $k_{obs} = 0.13 \pm 0.02$ $s^{-1}$ (published value[29] $0.16 \pm 0.02$ $s^{-1}$). Figure 3B illustrates the results obtained when oxygenated buffer was mixed with $H_2B$ reconstituted $Fe^{II}$-$iNOS_{heme}$ premixed with compound **19**. Again the data fit well to an A → B

kinetic model, however, the protein showed a transition from an intermediate with a Soret absorbance at 414 nm ($Fe^{II}$) to a species at 396 nm ($Fe^{III}$), with a $k_{obs} = 0.0267 \pm 0.0006$. Unlike the sample containing L-arginine, there was no observable build up of a ferrous-oxy species when $iNOS_{heme}$ was premixed with compound **19**. The overall rate of $iNOS_{heme}$ oxidation when premixed with **19** is much slower (~20%) than when premixed with L-arginine. The absence of a detectable ferrous-oxy species with **19** suggests that the rate of oxidation under these conditions is limited by the ability of oxygen to bind in the iNOS active site. With L-arginine, oxygen binding occurs rapidly (no ferrous-unligated $iNOS_{heme}$ detected) after which the rate-limiting step is dissociation of superoxide from the heme. With compound **19**, however, oxygen binding is likely the rate-limiting step with superoxide dissociation occurring at a higher relative rate, preventing accumulation of the ferrous-oxy species. A possible explanation for these results is that when compound **19** binds to iNOS the $N^G$-amino or -2,2,2-trifluoroethyl group may be positioned in the active site in such a way so as to effectively interfere with oxygen binding due to steric crowding. This inhibition of iNOS-mediated NADPH consumption by **19** is reminiscent of another NOS inhibitor with similar properties, $N^G$-nitro-L-arginine (L-NNA).[31] Crytallographic studies have shown that when bound to the NOS active site, the nitro group of L-NNA is specifically located above the heme cofactor, likely preventing productive oxygen binding.[32] Like compound **19**, $N^G$-nitro-L-arginine inhibits NO production by competing for the L-arginine binding site while also limiting the production of reactive oxygen species by shutting off NADPH consumption. These properties are unique and likely important in designing therapeutically useful NOS inhibitors that can prevent both the formation of NO and the formation of potentially damaging reactive oxygen species.

From the results obtained, it is apparent that the electon-rich/poor nature, as well as the location of substituents on the $N^G$-aminoguanidine center in the L-arginine analogues studied, dictates the nature and mechanism of NOS inhibition observed. While the four compounds investigated share the L-arginine amino acid scaffold, different inhibitory activities are observed with each species. Further study, employing a broader range of substituted $N^G$-aminoguanidines (now readily available using the synthetic methodology described here), is likely to provide a basis upon which the different inhibitory behaviors observed with this class of NOS inhibitors may be rationalized.

## Conclusion

In summary, we have developed a high-yielding methodology for the preparation of $N^G$-aminoguanidines that avoids the use of toxic reagents and harsh reaction conditions. This method was successfully applied to a number of examples, including the synthesis of four L-arginine-based inhibitors of iNOS. The mode of inhibition by these compounds was investigated and shown to be different depending upon the nature of the substituents present on the $N^G$-aminoguanidine moiety. While covalent modification of the heme cofactor plays a role in the time-dependent inactivation of iNOS by $N^G$-amino-L-arginine **16**, this is not a general mechanism for all $N^G$-aminoguanidines. Compound **18** was shown to irreversibly inactivate iNOS by a different mechanism and future efforts will be aimed at establishing the nature of this inactivation. Furthermore, one of the four compounds prepared, $N^G$-amino-$N^G$-2,2,2-trifluoroethyl-L-arginine **19**, was shown to be a competitive inhibitor of iNOS that also inhibits enzymatic NADPH consumption by interfering with oxygen binding. Further investigations into the isoform selective inhibition of NOS by compound **19** as well as crystallographic investigations into its mode of binding at the enzyme active site are warranted.

## Experimental Section

All reagents employed were of American Chemical Society (ACS) grade or finer and were used without further purification unless otherwise stated. CbzNCS was prepared as described in the literature.[23] Melting points are uncorrected and were determined on a Büchi oil immersion apparatus using open capillary tubes. $^1$H NMR, $^{13}$C NMR, and $^{19}$F NMR spectra were obtained on a Bruker AVQ-400 spectrometer. High-resolution FAB and ESI mass spectra were obtained using VG ZAB2-EQ and Q-Tof Premier (Waters) instruments, respectively. Microanalyses were obtained using a Perkin-Elmer 2400 Series II combustion analyzer. Optical rotations were recorded at 20 °C using a Perkin Elmer 241 polarimeter. $^1$H and $^{13}$C NMR spectra for compounds **16–19** are provided in Supporting Information.

**(*Z*)-Benzyl 2-((Benzylamino)(benzyloxycarbonylamino) methylene)hydrazinecarboxylate (1).** Benzylamine (0.5 mmol, 54 mg, 55 μL) was dissolved in $CH_2Cl_2$ (5.0 mL) and treated with CbzNCS (~1.0 mL of a 0.5 M solution in $CH_2Cl_2$) at room temperature until consumption of the amine was complete (typically within minutes), as evidenced by ninhydrin visualized TLC analysis. The mixture, now containing the thiourea intermediate, was then treated with $NEt_3$ (1.1 equiv, 0.55 mmol, 56 mg, 77 μL), EDCI (1.1 equiv, 0.55 mmol, 105 mg), and benzyl carbazate (1.1 equiv, 0.55 mmol, 91 mg). After one hour, TLC analysis (2:1 hexane/ethyl acetate) indicated formation of the desired product ($R_f = 0.35$) with residual thiourea ($R_f = 0.65$) still present. An additional 1.1 equiv of each reagent was added, and after stirring for another hour, the thiourea was completely consumed. The mixture was then washed with 0.1 M HCl (2 × 5 mL), $H_2O$ (2 × 5 mL) and brine (2 × 5 mL). The organic layer was dried over $Na_2SO_4$ followed by evaporation under vacuum. The residue was applied to a silica column and eluted with 2:1→1:1 hexane/ethyl acetate, yielding the desired product as a white solid (210 mg, 97%). Mp 116–118 °C; $^1$H NMR ($CDCl_3$, 400 MHz) δ 7.34–7.22 (m, 15H), 5.08 (s, 2H), 5.05 (s, 2H), 4.89 (s, 2H); $^{13}$C NMR ($CDCl_3$, 100 MHz) δ 156.4, 137.3, 135.3, 128.7, 128.6, 128.4, 128.2, 127.6, 127.55, 68.0, 67.5, 45.0; HRMS (FAB, M + H) calcd for $C_{24}H_{25}N_4O_4$, 433.1876; found, 433.1867; Anal. ($C_{24}H_{24}N_4O_4$) C, H, N.

**(*Z*)-Benzyl 2-((Benzyloxycarbonylamino)(cyclopentylamino) methylene)hydrazinecarboxylate (2).** Compound **2** was prepared as described above for compound **1**. Product obtained as a white solid (95%). Mp 118–120 °C; $^1$H NMR ($CDCl_3$, 400 MHz) δ 7.38–7.27 (m, 10H), 5.10 (s, 2H), 5.09 (s, 2H), 4.13 (m, 1H), 1.95–1.90 (m, 2H), 1.61–1.53 (m, 4H), 1.35–1.26 (m, 2H); $^{13}$C NMR ($CDCl_3$, 100 MHz) δ 159.8, 156.6, 137.0, 135.5, 128.5, 128.4, 128.1, 127.9, 67.8, 67.1, 52.4, 33.0, 23.5; HRMS (FAB, M + H) calcd for $C_{22}H_{27}N_4O_4$, 411.2032; found, 411.2040; Anal. ($C_{22}H_{26}N_4O_4$) C, H, N.

**(*Z*)-Benzyl 2-((Benzyloxycarbonylamino)(*tert*-butylamino) methylene)hydrazinecarboxylate (3).** Compound **3** was prepared as described above for compound **1**. Product obtained as a sticky foam (94%). $^1$H NMR ($CDCl_3$, 400 MHz) δ 7.38–7.27 (m, 10H), 5.14–5.12 (m, 4H), 1.39 (s, 9H); $^{13}$C NMR ($CDCl_3$, 100 MHz) δ 156.6, 135.6, 128.5, 128.43, 128.36, 128.1, 128.0, 67.8, 67.6, 52.1, 29.0; HRMS (FAB, M + H) calcd for $C_{21}H_{27}N_4O_4$, 399.2032; found, 399.2039; Anal. ($C_{21}H_{26}N_4O_4$) C, H, N.

**(*Z*)-Benzyl 2-((Benzyloxycarbonylamino)(4-bromophenylamino) methylene)hydrazinecarboxylate (4).** Compound **4** was prepared as described above for compound **1**. Product obtained as a white solid (91%). Mp 131–133 °C; $^1$H NMR ($CDCl_3$, 400 MHz) δ 7.39–7.27 (m, 14H), 5.12 (s, 2H), 5.11 (s, 2H); $^{13}$C NMR ($CDCl_3$, 100 MHz) δ 156.6, 136.1, 135.5, 132.1, 128.85, 128.76, 128.60, 128.57, 128.42, 128.38, 128.2, 124.1, 117.7, 67.94, 67.88; HRMS (FAB, M + H) calcd for $C_{23}H_{22}N_4O_4Br$, 497.0824; found, 497.0821; Anal. ($C_{23}H_{21}N_4O_4Br$) C, H, N.

**(*Z*)-Benzyl 2-((Benzyloxycarbonylamino)(3,5-dimethylphenylamino)methylene) hydrazinecarboxylate (5).** Compound **5** was prepared as described above for compound **1**. Product obtained as a white solid (96%). Mp 127–129 °C; $^1$H NMR ($CDCl_3$, 400 MHz) $\delta$ 7.38–7.27 (m, 10H), 6.93 (s, 2 H), 6.81 (s, 1H), 5.12 (s, 2H), 5.11 (s, 2H), 2.27 (s, 6H); $^{13}$C NMR ($CDCl_3$, 100 MHz) $\delta$ 156.7, 139.2, 136.2, 135.7, 128.51, 128.46, 128.24, 128.19, 128.1, 128.0, 67.7, 67.5, 21.3; HRMS (FAB, M + H) calcd for $C_{25}H_{27}N_4O_4$, 447.2032; found, 447.2043; Anal. ($C_{25}H_{26}N_4O_4$) C, H, N.

**(*S*)-Benzyl 4-Benzyl-5-oxo-1*H*-imidazole-1,2(4*H*,5*H*)-diyldicarbamate (6).** Compound **6** was prepared as described above for compound **1**. Product obtained as a clear glass (89%). $^1$H NMR ($CDCl_3$, 400 MHz) $\delta$ 7.52–7.04 (m, 15H), 5.14–4.99 (m, 4H), 4.27 (m, 1H), 3.31 (m, 1H), 2.88 (m, 1H); $^{13}$C NMR ($CDCl_3$, 100 MHz) $\delta$ 170.1, 163.0, 160.3, 154.7, 136.3, 135.5, 134.9, 129.5, 129.3, 128.8, 128.6, 128.4, 128.0, 68.6, 67.9, 58.4, 38.0; HRMS (FAB, M + H) calcd for $C_{26}H_{25}N_4O_5$, 473.1825; found, 473.1819; Anal. ($C_{26}H_{24}N_4O_5$) C, H, N.

***N*-δ-*tert*-Butoxycarbonyl-*N*-α-benzyloxycarbonyl-L-ornithine Benzyl Ester (7).** *N*-α-Cbz-L-ornithine (5.0 g, 19.0 mmol) was stirred in methanol (30 mL) and treated with a 10% $NEt_3$ solution in methanol (30 mL) followed by $Boc_2O$ (8.2 g, 38.0 mmol). The mixture was warmed to 40 °C and stirred for one hour, at which point TLC indicated consumption of starting material. The methanol was removed under vacuum, and the residue was treated with 20 mL of dilute HCl (pH 2.5) on ice, followed by extraction with ethyl actetate (4 × 50 mL). The combined ethyl acetate layers were combined, washed with brine, and dried over $Na_2SO_4$, and the solvent was removed to yield the Boc-protected intermediate as a pale yellow oil, used without further purification. This material was then dissolved in acetonitrile (175 mL), treated with diisopropylamine (1.05 equiv, 20.0 mmol, 2.7 g, 3.6 mL), followed by benzyl bromide (1.05 equiv, 20.0 mmol, 3.7g, 2.6 mL), and left to stir at room temperature for 14 h. The solvent was next removed under vacuum and the residue was redissolved in ethyl acetate (250 mL), washed with water (4 × 100 mL) and brine (2 × 100 mL), and dried over $Na_2SO_4$. Following solvent removal, recrystallization from ethyl acetate/hexanes yielded **7** as a white solid (7.89 g, 91% over 2 steps). Mp 107–109 °C; $^1$H NMR ($CDCl_3$, 400 MHz) $\delta$ 7.42–7.28 (m, 10H), 5.44 (br d, $J$ = 7.6 Hz, 1H), 5.29–5.11 (m, 4H), 4.52 (br s, 1H), 4.44 (m, 1H), 3.08 (m, 2H), 1.88 (m, 1H), 1.67 (m, 1H), 1.56–1.40 (m, 11H); $^{13}$C NMR ($CDCl_3$, 100 MHz) $\delta$ 172.1, 155.9, 136.2, 135.2, 128.6, 128.5, 128.3, 128.2, 128.1, 79.2, 67.2, 67.0, 53.6, 39.9, 29.9, 28.4, 25.9; HRMS (FAB, M + H) calcd for $C_{25}H_{33}N_2O_6$, 457.2339; found, 457.2336; Anal. ($C_{25}H_{32}N_2O_6$) C, H, N.

***N*-Uriedo-benzyloxycarbonyl-*N*-α-benzyloxycarbonyl-L-thiocitrulline Benzyl Ester (8).** Compound **7** (5.0 g, 11.0 mmol) was treated with 1:1 TFA/$CH_2Cl_2$ (80 mL) and stirred at room temperature for 1 h. The mixture was then evaporated under vacuum and the residue was dissolved in $CH_2Cl_2$ (100 mL) and treated with $NEt_3$ to neutralize excess TFA. CbzNCS was next added dropwise (as a 0.5 M solution in $CH_2Cl_2$) until the amine intermediate was consumed. Following solvent removal, the crude material was applied to a silica gel column (2:1 hexanes/ethyl acetate) and **8** isolated as a colorless oil **9** (4.9 g, 82%). $^1$H NMR ($CDCl_3$, 400 MHz) $\delta$ 9.63 (br s, 1H), 8.21 (br s, 1H), 7.42–7.28 (m, 15H), 5.44 (br d, $J$ = 8.0 Hz, 1H), 5.22–5.08 (m, 6H), 4.47 (m, 1H), 3.63 (m, 2H), 1.95–1.58 (m, 4H); $^{13}$C NMR ($CDCl_3$, 100 MHz) $\delta$ 179.1, 171.9, 155.9, 152.5, 136.1, 135.1, 134.5, 128.9, 128.8, 128.7, 128.5, 128.4, 128.3, 128.2, 128.1, 68.2, 67.4, 67.1, 53.5, 44.9, 30.0, 24.1; HRMS (FAB, M + H) calcd for $C_{29}H_{32}N_3O_6S$, 550.2012; found, 550.2002; Anal. ($C_{29}H_{31}N_3O_6S$) C, H, N.

***N*-Benzyloxycarbonyl-1-methylhydrazine Hydrochloride (9).** At room temperature, methyl hydrazine (10.0 mmol, 0.46 g, 0.53 mL) was dissolved in a mixture of $CH_2Cl_2$ (15 mL) and 1 M NaOH (15 mL) and treated with benzyl chloroformate (10.0 mmol, 1.7 g, 1.4 mL). The mixture was stirred rapidly for one hour, after which the layers were separated. The aqueous layer was extracted with an additional 20 mL of $CH_2Cl_2$, and the combined organic layers were dried over $Na_2SO_4$ and evaporated to yield a colorless oil. The HCl salt was prepared by dissolving the residue in methanol (5 mL) followed by dropwise addition of 1.25 M HCl in methanol (10 mL). The methanol was then removed under vacuum, and the product was obtained as white needles by recrystallization from isopropyl alcohol/diethyl ether (1.7 g, 78%). Mp 166–168 °C; $^1$H NMR (DMSO-$d_6$, 400 MHz) $\delta$ 7.43–7.28 (m, 5H), 5.17 (s, 2H), 3.15 (s, 3H); $^{13}$C NMR (DMSO-$d_6$, 100 MHz) $\delta$ 155.4, 136.0, 128.9, 128.7, 128.3, 68.4, 36.2; HRMS (FAB, M + H) calcd for $C_9H_{13}N_2O_2$, 181.0977; found, 181.0976; Anal. ($C_9H_{13}N_2O_2Cl$) C, H, N.

***N*-Benzyloxycarbonyl-2-methylhydrazine Hydrochloride (10).** At room temperature, methyl hydrazine (26.0 mmol, 1.2 g, 1.4 mL) and $Boc_2O$ (19.8 mmol, 4.3 g) were combined in methanol (25 mL). After stirring for 30 min, the solvent was removed under vacuum, and the residue was dissolved in a mixture of $CH_2Cl_2$ (20 mL) and 1 M NaOH (20 mL). While stirring rapidly, benzyl chloroformate (20.0 mmol, 3.4 g, 2.8 mL) was added. After stirring for one hour, the layers were separated and the organic layer was washed with 1 M HCl (2 × 15 mL), $H_2O$ (2 × 15 mL), and brine (2 × 15 mL) and dried over $Na_2SO_4$. The solvent was removed under vacuum and the residue was dissolved in methanol (40 mL), chilled on ice, and treated with acetyl chloride (10 mL). After stirring for 20 min, the mixture was concentrated under vacuum and the product was obtained as white needles by recrystallization from isopropyl alcohol (3.3 g, 77%). Mp 175–177 °C; $^1$H NMR (DMSO-$d_6$, 400 MHz) $\delta$ 7.39–7.28 (m, 5H), 5.15 (s, 2H), 2.70 (s, 3H); $^{13}$C NMR (DMSO-$d_6$, 100 MHz) $\delta$ 155.2, 136.0, 128.9, 128.7, 128.5, 67.6, 35.9; HRMS (FAB, M + H) calcd for $C_9H_{13}N_2O_2$, 181.0977; found, 181.0981; Anal. ($C_9H_{13}N_2O_2Cl$) C, H, N.

***N*-Benzyloxycarbonyl-2-(2,2,2-trifluoroethyl) Hydrazine (11).** On ice, 2,2,2-trifluoroethyl hydrazine (10.0 mmol, 1.63 g of a 70% by weight solution in water) was dissolved in a mixture of $CH_2Cl_2$ (15 mL) and 1 M NaOH (15 mL) and treated with benzyl chloroformate (10.0 mmol, 1.7 g, 1.4 mL). The mixture was stirred rapidly at room temperature for 6 h, after which the layers were separated. The aqueous layer was extracted with an additional 20 mL of $CH_2Cl_2$ and the combined organic layers were dried over $Na_2SO_4$ and evaporated to yield a white solid. Compound **11** was obtained as the free base by recrystallization from ethyl acetate/hexanes (1.91 g, 77%). Mp 79–81 °C; $^1$H NMR ($CDCl_3$, 400 MHz) $\delta$ 7.45–7.30 (m, 5H), 6.73 (br s, 1 H), 5.16 (s, 2H), 4.38 (br s, 1H), 3.43 (m, 2H); $^{13}$C NMR ($CDCl_3$, 100 MHz) $\delta$ 157.2, 135.6, 128.6, 128.5, 128.2, 124.8 (q, $J_{CF}$ = 278.0 Hz), 67.5, 52.7 (q, $J_{CF}$ = 30.3 Hz); $^{19}$F NMR ($CDCl_3$, 376.5 MHz) $\delta$ −70.9 (t, $J_{FH}$ = 9.1 Hz); HRMS (FAB, M + H) calcd for $C_{10}H_{12}N_2O_2F_3$, 249.0851; found, 249.0856; Anal. ($C_{10}H_{12}N_2O_2F_3$) C, H, N.

***N*$^G$-Benzyloxycarbonylamino-*N*$^{G'}$-benzyloxycarbonyl-*N*-α-benzyloxycarbonyl-L-arginine Benzyl Ester (12).** Thiourea **8** (0.5 mmol, 275 mg) was dissolved in $CH_2Cl_2$ (5.0 mL) and treated with $NEt_3$ (1.1 equiv, 0.55 mmol, 56 mg, 77 μL), EDCI (1.1 equiv, 0.55 mmol, 105 mg), and benzyl carbazate (1.1 equiv, 0.55 mmol, 91 mg). After one hour, TLC analysis (3:1 hexane/ethyl acetate) indicated formation of the desired product ($R_f$ = 0.30) with residual thiourea ($R_f$ = 0.6) still present. An additional 1.1 equiv of each reagent was added, and after stirring for another hour, the thiourea was completely consumed. The mixture was then washed with 0.1 M HCl (2 × 5 mL), $H_2O$ (2 × 5 mL), and brine (2 × 5 mL). The organic layer was dried over $Na_2SO_4$, followed by evaporation under vacuum. The residue was applied to a silica column and eluted with 3:2 hexane/ethyl acetate, yielding the desired product as an oil (310 mg, 91%). $^1$H NMR ($CDCl_3$, 400 MHz) $\delta$ 10.15 (br s, 1H), 7.42–7.21 (m, 20H), 5.95–5.56 (br m, 2H), 5.20–5.00 (m, 8H), 4.35 (m, 1H), 3.25 (m, 2H), 1.90–1.37 (m, 4H); $^{13}$C NMR ($CDCl_3$, 100 MHz) $\delta$ 172.1, 163.5, 160.8, 156.2, 137.2, 136.1, 135.3, 135.2, 128.62, 128.58, 128.5, 128.3, 128.2, 128.1, 127.7, 68.0, 67.2, 67.0, 53.6, 40.1, 29.5, 25.2; HRMS (FAB, M + H) calcd for $C_{37}H_{40}N_5O_8$, 682.2877; found, 682.2872; Anal. ($C_{37}H_{39}N_5O_8$) C, H, N.

***N*$^G$-Benzyloxycarbonylmethylamino-*N*$^{G'}$-benzyloxycarbonyl-*N*-α-benzyloxycarbonyl-L-arginine Benzyl Ester (13).** Compound **13** was prepared and purified as described above for **12** using Cbz-protected methyl hydrazine **9** in place of benzyl carbazate. Product

isolated as an oil (313 mg, 90%). $^1$H NMR ($CDCl_3$, 400 MHz) $\delta$ 10.40 (br s, 1H), 7.44–7.24 (m, 20H), 5.61 (br m, 1H), 5.20–5.03 (m, 8H), 4.38 (m, 1H), 3.35 (br m, 2H), 3.12 (s, 3H), 1.93–1.41 (m, 4H); $^{13}$C NMR ($CDCl_3$, 100 MHz) $\delta$ 172.0, 163.6, 159.8, 156.4, 156.0, 153.0, 137.3, 136.1, 135.5, 135.1, 128.64, 128.57, 128.5, 128.4, 128.3, 128.2, 128.1, 128.0, 127.7, 68.4, 67.3, 67.0, 53.4, 40.1, 38.4, 29.7, 25.3; HRMS (FAB, M + H) calcd for $C_{38}H_{42}N_5O_8$, 696.3033; found, 696.3036; Anal. ($C_{38}H_{41}N_5O_8$) C, H, N.

***N*$^G$-Benzyloxycarbonylamino-*N*$^G$-methyl-*N*$^{G'}$-benzyloxycarbonyl-*N*-α-benzyloxycarbonyl-L-arginine Benzyl Ester (14).** Compound **14** was prepared as described above for **12** using Cbz-protected methyl hydrazine **10** in place of benzyl carbazate. Chromatographic purification of the product required a much more polar solvent system (1:1 hexane/ethyl acetate → 5% methanol in chloroform) after which **14** was isolated as an oil (278 mg, 80%). $^1$H NMR ($CDCl_3$, 400 MHz) $\delta$ 8.01 (br s, 1H), 7.43–7.22 (m, 20H), 5.62 (br m, 1H), 5.19–5.03 (m, 8H), 4.33 (m, 1H), 3.24–3.01 (m, 5H), 1.85–1.36 (m, 4H); $^{13}$C NMR ($CDCl_3$, 100 MHz) $\delta$ 172.0, 160.2, 156.2, 155.1, 136.7, 136.1, 135.3, 135.2, 128.6, 128.53, 128.50, 128.46, 128.42, 128.37, 128.3, 128.5, 128.08, 128.0, 68.0, 67.6, 67.2, 67.0, 53.6, 43.5, 39.9, 29.3, 25.3; HRMS (FAB, M + H) calcd for $C_{38}H_{42}N_5O_8$, 696.3033; found, 696.3029; Anal. ($C_{38}H_{41}N_5O_8$) C, H, N.

***N*$^G$-Benzyloxycarbonyl-*N*$^G$-2,2,2-trifluoroethylamino-*N*$^{G'}$-benzyloxycarbonyl-*N*-α-benzyloxycarbonyl-L-arginine Benzyl Ester (15).** Compound **15** was prepared and purified as described above for **12** using Cbz-protected 2,2,2-trifluoromethyl hydrazine **11** in place of benzyl carbazate. The product was isolated as an oil (330 mg, 87%). $^1$H NMR ($CDCl_3$, 400 MHz) $\delta$ 8.06 (br s, 1H), 7.45–7.20 (m, 20H), 5.58 (br m, 1H), 5.20–4.99 (m, 8H), 4.13 (m, 1H), 3.49 (br m, 2H), 3.28–2.95 (br m, 2H), 1.85–1.37 (m, 4H); $^{13}$C NMR ($CDCl_3$, 100 MHz) $\delta$ 172.0, 161.7, 156.4, 154.4, 154.0, 136.9, 136.0, 135.1, 135.0, 128.7, 128.6, 128.5, 128.4, 128.34, 128.26, 128.21, 128.15, 128.1, 127.9, 124.2 (q, $J_{CF}$ = 279.7 Hz), 68.2, 67.4, 67.3, 53.2, 50.3 (br m), 43.9, 29.9, 25.1; $^{19}$F NMR ($CDCl_3$, 376.5 MHz) $\delta$ −69.2; HRMS (FAB, M + H) calcd for $C_{39}H_{41}N_5O_8F_3$, 764.2907; found, 764.2904; Anal. ($C_{39}H_{40}N_5O_8F_3$) C, H, N.

***N*$^G$-Amino-L-arginine Acetate (16).** Compound **12** (200 mg, 0.29 mmol) was dissolved in 10 mL of 1:1 methanol/$H_2O$ (1% acetic acid), and the system was purged with $N_2$(g) prior to addition of 10% Pd/C (100 mg). Hydrogen gas was delivered with a balloon to the stirring reaction mixture throughout the course of the reaction (5 h, room temperature). Following reaction completion, the catalyst was removed by filtering through Celite and washed with several volumes of MeOH/$H_2O$ (1% acetic acid). The filtrate was concentrated under vacuum and lyophilized to yield the amino acid monoacetate salt as a clear glass (72 mg, 98%). $^1$H NMR ($D_2O$, 400 MHz) $\delta$ 3.69 (t, $J$ = 6.1 Hz, 1H), 3.19 (t, $J$ = 6.9 Hz, 2H), 1.86–1.78 (m, 2H), 1.73–1.50 (m, 2H); $^{13}$C NMR ($D_2O$, 100 MHz) $\delta$ 180.6 (AcOH), 174.4, 157.9, 54.3, 40.1, 27.5, 24.0, 22.7 (AcOH); $[\alpha]_D$ = +15.3° (*c* 0.8, $H_2O$), lit.[33] +7.4° (*c* 0.46, MeOH); HRMS (FAB, M + H) calcd for $C_6H_{16}N_5O_2$, 190.1304; found, 190.1303; Anal. ($C_6H_{15}N_5O_2 \cdot 1.4AcOH \cdot 0.3H_2O$) C, H, N.

***N*$^G$-Methylamino-L-arginine Acetate (17).** Compound **17** was prepared from **13** as described above for **16**. The product was lyophilized to yield the amino acid monoacetate salt as a clear glass (99%). $^1$H NMR ($D_2O$, 400 MHz) $\delta$ 3.67 (t, $J$ = 6.1 Hz, 1H), 3.17 (t, $J$ = 6.9 Hz, 2H), 2.45 (s, 3H), 1.85–1.77 (m, 2H), 1.70–1.48 (m, 2H); $^{13}$C NMR ($D_2O$, 100 MHz) $\delta$ 180.5 (AcOH), 174.3, 156.9, 54.3, 40.1, 37.6, 27.5, 24.0, 22.8 (AcOH); $[\alpha]_D$ = +9.6° (*c* 0.8, $H_2O$); HRMS (FAB, M + H) calcd for $C_7H_{18}N_5O_2$, 204.1461; found, 204.1460; Anal. ($C_7H_{17}N_5O_2 \cdot 1.1AcOH \cdot 0.5H_2O$) C, H, N.

***N*$^G$-Amino-*N*$^G$-methyl-L-arginine (18).** Compound **18** was prepared from **14** as described above for **16**. The product was lyophilized to yield the amino acid with only trace acetic acid (evidenced by NMR) as a clear glass (94%). The lyophilized material is extremely hygroscopic, preventing satisfactory C, H, N analysis. $^1$H NMR ($D_2O$, 400 MHz) $\delta$ 4.05 (t, $J$ = 6.2 Hz, 1H), 3.25 (t, $J$ = 6.8 Hz, 2H), 3.17 (s, 3H), 2.01–1.86 (m, 2H), 1.81–1.58 (m, 2H); $^{13}$C NMR ($D_2O$, 100 MHz) $\delta$ 171.9, 157.2, 52.6, 40.7, 39.6, 26.9, 23.9; $[\alpha]_D$ = +28.5° (*c* 0.7, $H_2O$); HRMS (FAB, M + H) calcd for $C_7H_{18}N_5O_2$, 204.1461; found, 204.1464.

***N*$^G$-Amino-*N*$^G$-2,2,2-trifluoroethyl-L-arginine Acetate (19).** Compound **19** was prepared from **15** as described above for **16**. The product was lyophilized to yield the amino acid monoacetate salt as a clear glass (95%). $^1$H NMR ($D_2O$, 400 MHz) $\delta$ 4.28 (q, $J_{HF}$ = 8.6 Hz, 2H), 3.70 (t, $J$ = 6.1 Hz, 1H), 3.27 (t, $J$ = 7.0 Hz, 3H), 1.87–1.77 (m, 2H), 1.75–1.54 (m, 2H); $^{13}$C NMR ($D_2O$, 100 MHz) $\delta$ 180.1 (AcOH), 174.3, 157.5, 123.9 (q, $J_{CF}$ = 280.5 Hz), 54.2, 52.7 (q, $J_{CF}$ = 33.2 Hz), 41.1, 27.5, 23.7, 22.5 (AcOH); $^{19}$F-NMR ($D_2O$, 376.5 MHz) $\delta$ −69.6 (t, $J_{FH}$ = 8.4 Hz); $[\alpha]_D$ = +20.7° (*c* 0.9, $H_2O$); HRMS (FAB, M + H) calcd for $C_8H_{17}N_5O_2F_3$, 272.1334; found, 272.1333; Anal. ($C_8H_{16}N_5O_2F_3 \cdot 1.4AcOH \cdot 0.2H_2O$) C, H, N.

**Spectral $K_d$ Titrations.** $iNOS_{heme}$ was expressed and purified as previously described.[25] In a typical assay, $H_4B$-bound $iNOS_{heme}$ (500 μL of 0.5–1 μM) was titrated with the compound of choice, working at concentrations appropriate to detect the spectral transition from 418 nm ($Fe^{III}$-aqua) to 394 nm ($Fe^{III}$-unligated). Absorbance spectra were corrected for the dilution due to the volume of titrant added. As described in the text, absorbance changes ($\Delta\Delta Abs = \Delta Abs_{394} - \Delta Abs_{418}$) were plotted as a function of compound concentration and the $K_d$ was determined by fitting the data by a nonlinear least-squares fit to the saturation binding equation: $\Delta\Delta Abs = (\Delta\Delta Abs_{max} \times [compound])/(K_d + [compound])$ (KaleidaGraph, Abelbeck Software). All analyses were performed in triplicate and the average value ± the standard deviation reported.

**iNOS Inhibition Assays.** A modified, high-throughput oxymyoglobin assay[34] using a 96-well plate reader was utilized to assess the inhibition exhibited by compounds **16**–**19** with full-length iNOS. Described here is the $K_i$ determination for **19**. Assay reactions were prepared containing L-arginine (0, 10, 20, 50, 100, 200, 400, and 1000 μM), **19** (30, 60, 90, and 120 μM), 12 μM $H_4B$, 150 μM DTT, 8.5 μM oxymyoglobin, and 15 nM iNOS in 100 mM HEPES (pH 7.5). The NOS reaction was initiated by addition of NADPH (final concentration 100 μM) to each well using a multichannel pipet. NO production was monitored by measuring the increase in absorbance at 405 nm, corresponding to the NO-mediated conversion of oxymyoglobin to metmyoglobin. The data derived from the Michaelis–Menten plots of iNOS inhibition by **19** was used to generate an apparent $K_m$ versus [**19**] replot from which the $K_i$ for **19** was determined to be 10.5 ± 5.7 μM. Each analysis was performed in triplicate and the average reported along with the associated error in each fit.

**Time-Dependent Inactivation of iNOS.** An assay using a 96-well plate reader was utilized to assess the time-dependent inactivation of iNOS exhibited by compounds **16**–**19**. Described here is the $K_{inactivation}$ determination for **18**. Inactivation was initiated by adding **18** (300 μM) to a solution containing 100 mM HEPES (pH 7.5), 150 nM iNOS, 27 μM $H_4B$, 345 μM DTT, 12 μM oxyMb, and 100 μM NADPH. Inactivation of iNOS was terminated at different time points (0–5.0 min) by transferring 30 μL of the inactivation mixture to 270 μL of a reaction solution containing 100 mM HEPES (pH 7.5), 1.0 mM L-arginine, 27 μM $H_4B$, 345 μM DTT, 12 μM oxyMb, and 100 μM NADPH. NO production was monitored at 405 nm, as described for the previous kinetic assays.

**Inhibition of iNOS-Mediated NADPH Oxidation.** Compounds **17** and **19** were investigated for their ability to prevent iNOS-mediated NADPH oxidation. A solution containing 100 mM HEPES pH 7.5, 1.0 mM inhibitor, 80 nM iNOS, 2.6 μM $H_4B$, 30 μM DTT, and 100 μM NADPH (final volume 450 μL) was added to a quartz cuvette. The conversion of NADPH to $NADP^+$ was monitored spectrally at 340 nm using a Cary 3E UV–visible spectrophotometer for 5.0 min.

**Stopped-Flow UV–Visible Spectroscopic Analysis.** $iNOS_{heme}$ oxidation was measured on a Hi-Tech Scientific SF-61 stopped-flow spectrophotometer equipped with a Neslab RTE-100 temperature controller set at 4 °C. Directly before use, $iNOS_{heme}$ was desalted into 100 mM HEPES (pH 7.5), followed by addition of $H_2B$ (400 μM) and DTT (5 mM). The sample was monitored

spectrally until no further change was observed, indicating complete reconstitution with the $H_2B$. The protein was transferred into a Coy anaerobic glovebag and allowed to sit at 4 °C for >1 h to equilibrate the reconstituted protein in an $O_2$-free environment. An aliquot of the protein (200 $\mu$L) was then reduced with sodium dithionite (50 $\mu$M) and mixed with either L-arginine or compound **19** (10 mM) and 100 mM HEPES (pH 7.5) to give a final volume of 1.0 mL. The protein was rapidly mixed with an equal volume of a solution of $O_2$-saturated buffer (2.2 mM). The system had been previously scrubbed of oxygen with a solution of 500 $\mu$M sodium dithionite in 100 mM HEPES (pH 7.5). After mixing, the sample was monitored spectrally from 350–650 nm. Final solution concentrations consisted of $iNOS_{heme}$ (2–4 $\mu$M), $H_2B$ (50–100 $\mu$M), DTT (50–125 $\mu$M), L-arginine or compound **19** (5 mM), and $O_2$ (1.1 mM). All data was fit with Specfit global analysis software from Spectrum Software Associates (Chapel Hill, NC, USA).

**Acknowledgment.** This work was supported by the Aldo DeBenedictis Fund, the Natural Sciences and Engineering Council of Canada, and the Alberta Heritage Foundation for Medical Research (postdoctoral fellowships to N.I.M.). Nathaniel Fernhoff and Michelle Chang are gratefully acknowledged for providing full-length iNOS.

**Supporting Information Available:** $^1H$ and $^{13}C$ NMR spectra for compounds **16**–**19** and complete results of the spectral binding and inhibition assays for compounds **16**–**19**. This material is available free of charge via the Internet at http://pubs.acs.org.

## References

(1) T'Ang, A.; Lien, E. J.; Lai, M. M. C. Optimization of the Schiff bases of *N*-hydroxy-*N*′-aminoguanidine as anticancer and antiviral agents. *J. Med. Chem.* **1985**, *28*, 1103–1106.
(2) Pignatello, R.; Panico, A.; Mazzone, P.; Pinizzotto, M. R.; Garozzo, A.; Fumeri, P. M. Schiff bases of *N*-hydroxy-*N*′-aminoguanidines as antiviral, antibacterial, and anticancer agents. *Eur. J. Med. Chem.* **1994**, *29*, 781.
(3) Augstein, J.; Green, S. M.; Katritzky, A. R.; Monro, A. M. The synthesis, proof of structure, and biological activity of some mono-substituted aminoguanidines. *J. Med. Chem.* **1965**, *8*, 395–397.
(4) Cerami, A.; Wagle, D. R.; Ulrich, P. C. Di- and tri-aminoguanidines and their use to inhibit the advanced glycosylation of proteins. U.S. Patent 96/040663, 1996.
(5) Ulrich, P. C.; Cerami, A. 2-Alkylidene-aminoguanidines for inhibiting advanced nonenzymatic glycosylation of proteins. U.S. Patent 92/19236, 1992.
(6) Bryant, H. U.; Nelson, D. L.; Button, D.; Cole, H. W.; Baez, M. B.; Lucaites, V. L.; Wainscott, D. B.; Whitesitt, C.; Reel, J.; Simon, R.; Koppel, G. A. A novel class of 5-HT2A receptor antagonists: aryl aminoguanidines. *Life Sci.* **1996**, *59*, 1259–1268.
(7) Lu, T.; Tomczuk, B. E.; Markotan, T. P.; Siedem, C. Heteroaryl aminoguanidines and alkoxyguanidines and their use as protease inhibitors. U.S. 04/7029654, 2004.
(8) Tomczuk, B. E.; Soll, R. M.; Lu, T.; Fedde, C. L.; Illig, C. R.; Markotan, T. P.; Stagnaro, T. P. Aminoguanidines and alkoxyguanidines as protease inhibitors. U.S. Patent 03/6706765, 2003.
(9) Wolff, D. J.; Gauld, D. S.; Neulander, M. J.; Southan, G. Inactivation of nitric oxide synthase by substituted aminoguanidines and aminoisothioureas. *J. Pharmacol. Exp. Ther.* **1997**, *283*, 265–273.
(10) Fukuto, J. M.; Wood, K. S.; Byrns, R. E.; Ignarro, L. J. $N^G$-amino-L-arginine: A new potent antagonist of L-arginine-mediated endothelium-dependent relaxation. *Biochem. Biophys. Res. Commun.* **1990**, *168*, 458–465.
(11) Griffith, O. W.; Stuehr, D. J. Nitric oxide synthases: Properties and catalytic mechanism. *Annu. Rev. Physiol.* **1995**, *57*, 707–736.
(12) Kerwin, J. F., Jr.; Lancaster, J. R., Jr.; Feldman, P. L. Nitric oxide: A new paradigm for second messengers. *J. Med. Chem.* **1995**, *38*, 4343–4362.
(13) Roman, L. J.; Martasek, P.; Masters, B. S. Intrinsic and extrinsic modulation of nitric oxide synthase activity. *Chem. Rev.* **2002**, *102*, 1179–1190.
(14) Alderton, W. K.; Cooper, C. E.; Knowles, R. G. Nitric oxide synthases: Structure, function, and inhibition. *Biochem. J.* **2001**, *357*, 593–615.
(15) Hobbs, A. J.; Higgs, A.; Moncada, S. Inhibition of nitric oxide synthase as a potential therapeutic target. *Annu. Rev. Pharmacol. Toxicol.* **1999**, *39*, 191–220.
(16) Belzecki, C.; Hintze, B.; Kwiatkowska, K. *Bull. Acad. Pol. Sci.* **1970**, *18*, 375–378.
(17) Lieber, E.; Smith, G. B. L. The chemistry of aminoguanidine and related substances. *Chem. Rev.* **1939**, *25*, 213–271.
(18) Lakhan, R.; Sharma, B. P.; Shukla, B. N. Synthesis and antimicrobial activity of 1-aryl-2-amino-3-(4-arylthiazol-2-yl)/(benzothiazol-2-yl)guanidines. *Farmaco* **2000**, *55*, 331–337.
(19) Hunig, S.; Muller, F. AZOFARBSTOFFE DURCH OXYDATIVE KUPPLUNG, XXI. Kupplung nicht-aromatischer Amidrazone und ω-Benzolsulfonyl-amidrazone. *Liebigs Ann. Chem.* **1962**, *651*, 73–89.
(20) Katritzky, A. R.; Khashab, N. M.; Bobrov, S.; Yoshioka, M. Synthesis of mono- and symmetrical di-*N*-hydroxy- and *N*-aminoguanidines. *J. Org. Chem.* **2006**, *71*, 6753–6758.
(21) Wolff, D. J.; Lubeskie, A. Inactivation of nitric oxide synthase isoforms by diaminoguanidine and $N^G$-amino-L-arginine. *Arch. Biochem. Biophys.* **1996**, *325*, 227–234.
(22) Vuletich, J. L.; Lowe, E. R.; Jianmongkol, S.; Kamada, Y.; Kent, U. M.; Bender, A. T.; Demady, D. R.; Hollenberg, P. F.; Osawa, Y. Alteration of the heme prosthetic group of neuronal nitric-oxide synthase during inactivation by $N^G$-amino-L-arginine in vitro and in vivo. *Mol. Pharmacol.* **2002**, *62*, 110–118.
(23) Martin, N. I.; Woodward, J. J.; Marletta, M. A. $N^G$-Hydroxyguanidines from primary amines. *Org. Lett.* **2006**, *8*, 4035–4038.
(24) Poss, M. A.; Iwanowicz, E.; Reid, J. A.; Lin, J.; Gu, Z. A mild and efficient method for the preparation of guanidines. *Tetrahedron Lett.* **1992**, *33*, 5933.
(25) Hurshman, A. R.; Marletta, M. A. Reactions catalyzed by the heme domain of inducible nitric oxide synthase: evidence for the involvement of tetrahydrobiopterin in electron transfer. *Biochemistry* **2002**, *41*, 3439–3456.
(26) Komori, Y.; Wallace, G. C.; Fukuto, J. M. Inhibition of purified nitric oxide synthase from rat cerebellum and macrophage by L-arginine analogs. *Arch. Biochem. Biophys.* **1994**, *315*, 213–218.
(27) Abu-Soud, H. M.; Stuehr, D. J. Nitric oxide synthases reveal a role for calmodulin in controlling electron transfer. *Proc. Natl. Acad. Sci. U.S.A.* **1993**, *90*, 10769–10772.
(28) Abu-Soud, H. M.; Feldman, P. L.; Clark, P.; Stuehr, D. J. Electron transfer in the nitric-oxide synthases. Characterization of L-arginine analogs that block heme iron reduction. *J. Biol. Chem.* **1994**, *269*, 32318–32326.
(29) Lefevre-Groboillot, D.; Boucher, J. L.; Mansuy, D.; Stuehr, D. J. Reactivity of the heme-dioxygen complex of the inducible nitric oxide synthase in the presence of alternative substrates. *FEBS J.* **2006**, *273*, 180–191.
(30) Moreau, M.; Boucher, J. L.; Mattioli, T. A.; Stuehr, D. J.; Mansuy, D.; Santolini, J. Differential effects of alkyl- and arylguanidines on the stability and reactivity of inducible NOS heme-dioxygen complexes. *Biochemistry* **2006**, *45*, 3988–3999.
(31) Furfine, E. S.; Harmon, M. F.; Paith, J. E.; Garvey, E. P. Selective inhibition of constitutive nitric oxide synthase by L-$N^G$-nitroarginine. *Biochemistry* **1993**, *32*, 8512–8517.
(32) Raman, C. S.; Li, H.; Martasek, P.; Southan, G.; Masters, B. S.; Poulos, T. L. Crystal structure of nitric oxide synthase bound to nitro indazole reveals a novel inactivation mechanism. *Biochemistry* **2001**, *40*, 13448–13455.
(33) Wagenaar, F. L.; Kerwin, J. F. Methodology for the preparation of *N*-guanidino-modified arginines and related derivatives. *J. Org. Chem.* **1993**, *58*, 4331–4338.
(34) Dawson, J.; Knowles, R. G. A microtiter-plate assay of nitric oxide synthase activity. *Mol. Biotechnol.* **1999**, *12*, 275–279.

JM701119V